



All-optical mode-group multiplexed transmission over a graded-index ring-core fiber with single radial mode

FENG FENG,^{1,*} XIANQING JIN,² DOMINIC O'BRIEN,² FRANK PAYNE,² YONGMIN JUNG,³ QIONGYUE KANG,³ PRANABESH BARUA,³ JAYANTA K. SAHU,³ SHAI-UL ALAM,³ DAVID J. RICHARDSON,³ AND TIMOTHY D. WILKINSON¹

¹Electrical Division, Department of Engineering, University of Cambridge, 9 JJ Thomson Avenue, Cambridge, CB3 0FA, UK

²University of Oxford, Parks Road, Oxford, OX1 3PJ, UK

³Optoelectronics Research Centre, University of Southampton, Southampton, SO17 1BJ, UK
*ff263@cam.ac.uk

Abstract: We present a design of graded-index ring-core fiber (GI-RCF) supporting 3 linearly polarized (LP) mode-groups (i.e. LP₀₁, LP₁₁ and LP₂₁) with a single radial index of one for mode-division multiplexed (MDM) transmission. Reconfigurable spatial light modulator (SLM) based spatial (mode) (de)multiplexers are used to systematically characterize spatial/temporal modal properties of the GI-RCF. We also demonstrate all-optical mode-group multiplexed transmissions over a 360m fabricated GI-RCF without using multiple-input multiple-output digital signal processing (MIMO DSP).

Published by The Optical Society under the terms of the [Creative Commons Attribution 4.0 License](https://creativecommons.org/licenses/by/4.0/). Further distribution of this work must maintain attribution to the author(s) and the published article's title, journal citation, and DOI.

OCIS codes: (060.2330) Fiber optics communications; (060.2270) Fiber characterization; (060.4230) Multiplexing.

References and links

1. D. Richardson, J. Fini, and L. Nelson, "Space-division multiplexing in optical fibres," *Nat. Photonics* **7**(5), 354–362 (2013).
2. R. J. Essiambre, G. Kramer, P. J. Winzer, G. J. Foschini, and B. Goebel, "Capacity Limits of Optical Fiber Networks," *J. Lightwave Technol.* **28**(4), 662–701 (2010).
3. G. Li, N. Bai, N. Zhao, and C. Xia, "Space-division multiplexing: the next frontier in optical communication," *Adv. Opt. Photonics* **6**(4), 413–487 (2014).
4. N. K. Fontaine, R. Ryf, H. Chen, A. V. Benitez, B. Guan, R. Scott, B. Ercan, S. J. B. Yoo, L. E. Grüner-Nielsen, Y. Sun, R. Lingle, E. Antonio-Lopez, and R. Amezcua-Correa, "30×30 MIMO Transmission over 15 Spatial Modes," in *Optical Fiber Communication Conference Post Deadline Papers, OSA Technical Digest* (online) (Optical Society of America, 2015), paper Th5C.1.
5. P. Sillard, D. Molin, M. Bigot-Astruc, A. Amezcua-Correa, K. de Jongh, and F. Achten, "50 μm Multimode Fibers for Mode Division Multiplexing," *J. Lightwave Technol.* **34**(8), 1672–1677 (2016).
6. R. Ryf, N. K. Fontaine, B. Guan, B. Huang, M. Esmaelpour, S. Randel, A. H. Gnauck, S. Chandrasekhar, A. Adamiecki, G. Raybon, R. W. Tkach, R. Shubochkin, Y. Sun, and R. Lingle, Jr., "305-km combined wavelength and mode-multiplexed transmission over conventional graded-index multimode fibre." in *Proceedings of European Conference on Optical Communication* (2014), paper PD.3.5.
7. G. Labroille, P. Jian, L. Garcia, J. B. Trinel, R. Kassi, L. Bigot, and J. F. Morizur, "30 Gbit/s Transmission over 1 km of Conventional Multi-mode Fiber using Mode Group Multiplexing with OOK modulation and direct detection," in the *2015 European Conference and Exhibition on Optical Communication (ECOC)*, P.5.12.
8. G. Milione, E. Ip, M. J. Li, J. Stone, G. Peng, and T. Wang, "Mode crosstalk matrix measurement of a 1 km elliptical core few-mode optical fiber," *Opt. Lett.* **41**(12), 2755–2758 (2016).
9. E. Ip, G. Milione, M. J. Li, N. Cvijetic, K. Kanonakis, J. Stone, G. Peng, X. Prieto, C. Montero, V. Moreno, and J. Liñares, "SDM transmission of real-time 10GbE traffic using commercial SFP + transceivers over 0.5km elliptical-core few-mode fiber," *Opt. Express* **23**(13), 17120–17126 (2015).
10. G. Milione, P. N. Ji, E. Ip, M. Li, J. Stone, and G. Peng, "1.2Tb/s MIMO-less Transmission Over 1km of Four-Core Elliptical-Core-Few-Mode Fiber with s125-moron-Diameter Cladding," *21st Optoelectronics and Communication Conference, post-deadline paper*, 1–3, 2016.

11. G. Milione, P. N. Ji, E. Ip, M. Li, J. Stone, and G. Peng, "Real-time Bi-directional 10GbE Transmission using MIMO-less Space-division-multiplexing with Spatial Modes," in Optical Fiber Communication Conference, OSA Technical Digest (online) (Optical Society of America, 2016), paper W1F.2.
12. X. Jin, A. Gomez, K. Shi, B. C. Thomsen, F. Feng, G. S. D. Gordon, T. D. Wilkinson, Y. Jung, Q. Kang, P. Barua, J. Sahu, S. Alam, D. J. Richardson, D. C. O'Brien, and F. P. Payne, "Mode coupling effects in ring-core fibres for space-division multiplexed systems," *J. Lightwave Technol.* **34**(14), 3365–3372 (2016).
13. F. Feng, G. S. Gordon, X. Q. Jin, D. C. O'Brien, F. P. Payne, Y. Jung, Q. Kang, J. K. Sahu, S. U. Alam, D. J. Richardson, and T. D. Wilkinson, "Experimental Characterization of a Graded-Index Ring-Core Fiber Supporting 7 LP Mode Groups," in Optical Fiber Communication Conference, (2015), paper Tu2D.3.
14. F. Feng, X. Guo, G. S. Gordon, X. Jin, F. Payne, Y. Jung, Q. Kang, S. Alam, P. Barua, J. Sahu, D. J. Richardson, I. H. White, and T. D. Wilkinson, "All-optical Mode-Group Division Multiplexing Over a Graded-Index Ring-Core Fiber with Single Radial Mode," in Optical Fiber Communication Conference, OSA Technical Digest (online) (Optical Society of America, 2016), paper W3D.5.
15. Y. Jung, Q. Kang, H. Zhou, R. Zhang, S. Chen, H. Wang, Y. Yang, X. Jin, F. P. Payne, S. Alam, and D. J. Richardson, S. U. Alam, D. Richardson, "Low-Loss 25.3 km Few-Mode Ring-Core Fiber for Mode-Division Multiplexed Transmission," *J. Lightwave Technol.* **35**(8), 1363–1368 (2017).
16. C. R. Doerr, N. Fontaine, M. Hirano, T. Sasaki, L. Buhl, and P. Winzer, "Silicon photonic integrated circuit for coupling to a ring-core multimode fiber for space-division multiplexing," in 37th European Conference and Exposition on Optical Communications, (2011), paper Th.13.A.3.
17. H. Huang, G. Milione, M. P. J. Lavery, G. Xie, Y. Ren, Y. Cao, N. Ahmed, T. An Nguyen, D. A. Nolan, M. J. Li, M. Tur, R. R. Alfano, and A. E. Willner, "Mode division multiplexing using an orbital angular momentum mode sorter and MIMO-DSP over a graded-index few-mode optical fibre," *Sci. Rep.* **5**, 14931 (2015).
18. J. Carpenter, B. J. Eggleton, and J. Schröder, "110x110 optical mode transfer matrix inversion," *Opt. Express* **22**(1), 96–101 (2014).
19. J. Carpenter, B. C. Thomsen, and T. D. Wilkinson, "Degenerate Mode-Group Division Multiplexing," *J. Lightwave Technol.* **30**(24), 3946–3952 (2012).

1. Introduction

Mode-division multiplexing (MDM) in optical fibers, as one embodiment of space-division multiplexing (SDM), has been proposed to substantially increase transmission capacity per fiber by parallel exploiting multiple eigenmodes in a multimode fiber (MMF) as independent data channels, the goal of which is to overcome data capacity limit of current single-mode fiber systems imposed by nonlinear effects at reduced cost and energy consumption per bit transmitted [1,2]. For MDM to become a viable solution, research investigations and developments on several aspects are highly demanded. For example, they encompass customized MDM optical fibers with large (or small) effective index difference between mode-groups for weak (or strong) mode coupling, selective spatial mode (de)multiplexers, multiple-input multiple-output (MIMO) digital signal processing (DSP) to undo mode coupling with low computational complexity, as well as multimode counterpart components extended from single-mode fiber systems such as optical amplifiers and switches [3].

Mode coupling/crosstalk is one of the critical factors that limit the overall performance of MDM transmission systems. In general, MDM transmissions with strongly coupled spatial mode channels require full mode diversity coherent detection at the receiving end and MIMO DSP to recover independent data channels. To achieve practical real time operation and reasonable power consumption, reducing receiver computational complexity of MIMO DSP is essential. MIMO optimized MMFs with low differential group delays (DGD) and/or DGD management are often employed to lower the complexity of MIMO DSP complexity. In long distance transmission applications, spatial mode channels over the MDM links are strongly mixed (i.e. strongly coupled regime), and MIMO optimized MMFs and/or DGD management have been regarded as a promising solution for more practical receiver computational complexity of MIMO DSP [4–6]. On the other hand, mostly for short distance applications such as data center networks, spatial modes/mode-groups are weakly coupled or uncoupled by using customized MMFs with large DGD values and/or components, particularly mode selective spatial (de)multiplexers that barely generate modal crosstalk [7,8]. Weakly coupled regime could eliminate the use of coherent detection and MIMO DSP and enable using commercial direct detection transceivers, making weakly coupled MDM links very attractive

for data capacity upgrade at low cost and low power consumption while reducing cabling footprint mostly in short distance networks [9–11].

In this paper, a graded-index ring-core fiber (GI-RCF) supporting 3 linearly polarized (LP) mode-groups with single radial index was designed to have large effective index differences ($\geq 1 \times 10^{-3}$) that ensure low distributed mode coupling between mode-groups from the GI-RCF of at least 10km length. Meanwhile, relatively weak discrete mode coupling between all supported spatial mode-groups of the GI-RCF is also achieved by using mode-selective reconfigurable spatial light modulator (SLM) based spatial (de)multiplexers. We have experimentally demonstrated $3 \times 12.5\text{Gbit/s}$ and $2 \times 12.5\text{Gbit/s}$ all-optical mode-group multiplexed transmissions over a 360m fabricated GI-RCF using all guided 3 spatial mode-groups and 2 non-adjacent mode-groups of the GI-RCF with simple on-off keying (OOK) modulation and direct detection. Prior to the transmission experiments, we present the design of the GI-RCF and characterize spatial/temporal modal properties of the GI-RCF.

2. Ring core fiber design and characterization

2.1 Ring core fiber design

RCFs have been reported to be an attractive class of multimode fibers for MDM systems due to their unique features [12–15]. The number of modes supported by a RCF can be adjusted by changing the radius and thickness of the ring layer. To support a relatively large number of guided modes with a large average effective index difference that reduces mode couplings between mode-groups, RCFs are usually designed to support a single radial mode and multiple azimuthal modes. Because of their simpler pattern structures of spatial modes with a single radial index, selective ring mode excitation can be performed using a compact silicon photonic integrated circuit with a circular grating coupler fed by an array of waveguides, which has been demonstrated experimentally in [16]. Another demonstrated example of a mode (de)multiplexer for azimuthally varying spatial modes with a single radial index is an orbital angular momentum (OAM) mode sorter that consists of two refractive optical elements [17]. One unique feature that RCFs have is that the propagation constant difference between adjacent mode-groups increase significantly with increasing azimuthal index number of the modes. This feature results in relatively strong coupling between low order mode-groups but weak coupling between high order mode-groups. As a GI-RCF supporting 7 LP mode-groups reported in [13], low order four mode-groups of the fiber are strongly coupled and higher order mode-groups experience relatively weak coupling, aiming to adopt strongly coupled regime for low-order mode channels and weakly coupled regime for high-order mode channels within a certain transmission distance.

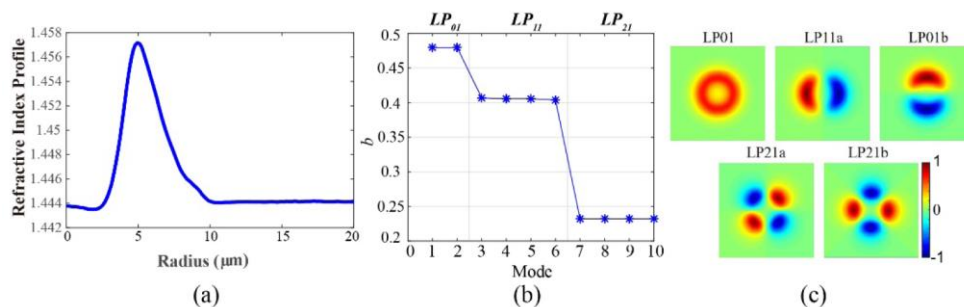


Fig. 1. (a) Refractive index profile of the GI RCF, (b) normalized propagation constants of vector modes and (c) theoretical mode field distributions of all guided LP modes in the RCF.

Figure 1(a)-(c) show the measured refractive index profile of GI-RCF used here, normalized propagation constants of vector modes and theoretical mode field distributions of all guided LP modes calculated using the refractive index profile. The GI-RCF supports three

LP mode-groups with a single radial index of one: LP_{01} , LP_{11} and LP_{21} . Each $LP_{l>0, m=1}$ mode has two-fold spatial degeneracy in each polarization, where l and m are the azimuthal and radial index respectively. These sets of degenerate modes form a mode group and mix heavily in the fiber, but mode coupling between mode groups is small.

2.2 Experimental characterization of the GI-RCF

We characterize modal properties of the GI-RCF using precise holographic mode excitation/detection enabled by reconfigurable SLM based spatial (de)multiplexers. The configuration of SLM based spatial (de)multiplexers is depicted in Fig. 2. Using a polarization diversity configuration, the SLM based spatial (de)multiplexers can accommodate any input polarization state. This configuration also allows launching and detecting each polarization mode individually. Figure 2 outlines the experimental system used to spatially resolve modal properties of the GI-RCF. We previously employed the system to characterize other RCF designs [13,14]. Each spatial/polarization mode supported by the GI-RCF is precisely excited and detected by programming corresponding phase masks (holograms) onto the SLM based spatial (de)multiplexers at both ends. The phase masks are generated using simulated annealing algorithm under the constraint of less than 1% error and maximum possible light conversion efficiency in a $70\mu\text{m}$ radius circle around the fiber core. Figure 3(b) shows the light conversion efficiency of the generated phase mask that converts a Gaussian beam illumination to each LP mode supported by the GI-RCF with the magnification of the used optical system. In the SLM based spatial multiplexer, the focal length of the collimating lens after SMF array is 15.3mm and the focal length of the refocusing lens before the RCF is 8.2mm. The mode field diameter of the Gaussian beam illumination on the SLM is 3.08 mm.

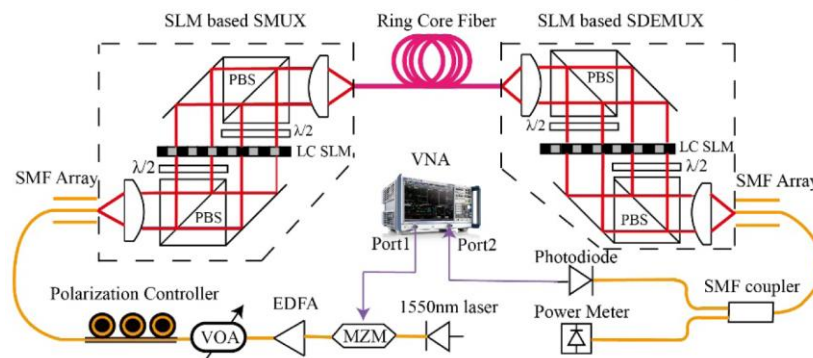


Fig. 2. Experimental system that modally characterizes the GI-RCF.

SLM based spatial (de)multiplexers support multiple MDM channels. For modal characterization of the fiber, only one channel that maps one input single mode fiber (SMF) port to one output SMF port is used. A polarization controller aligns the input polarization state to ensure it has approximately equal component along horizontal and vertical polarization axes of the system. The multiplexer SLM launches each mode of the GI-RCF in each polarization one at a time. For each mode launch in each polarization, the de-multiplexer SLM displays phase masks for each spatial mode in each polarization sequentially to decompose the received modal superposition. A vector network analyzer (VNA) with a frequency range from 40MHz to 20GHz measures frequency/time response for each pair of launch and detect spatial/polarization modes, producing a full 10×10 mode transfer matrix in the time domain. Figure 3(a) shows the measured temporal-domain mode transfer matrix aggregated over two launched and detected polarizations. In diagonal elements of the matrix colored in green, single dominant pulses arrive at different time correspond to different propagation modes supported by the GI-RCF. As shown in Fig. 3(c), the measured DGD

values are closely matched to the theoretical values calculated from the refractive index profile of the fiber. From the measured temporal-domain mode transfer matrix, we can separately analyze the mode couplings/crosstalk occurred in the system based on their locations, such as discrete modal crosstalk at spatial multiplexers and distributed mode coupling from the fiber itself.

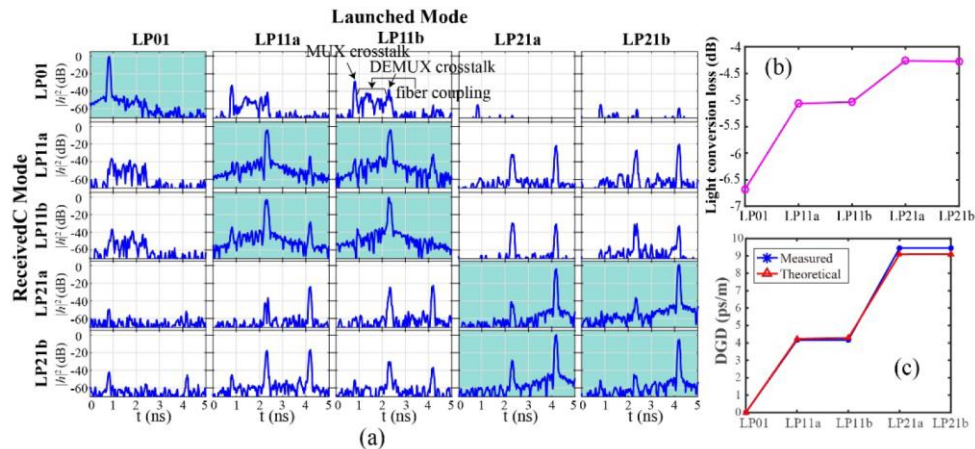


Fig. 3. (a) Measured temporal-domain mode transfer matrix (summed over polarizations) of the 360 m GI-RCF. (b) Light conversion loss of the generated phase masks for the LP modes supported by the GI-RCF. (c) Comparison between measured DGDs and designed DGD values of the GI-RCF.

In each cell of the matrix, multiple discrete impulse peaks indicate discrete modal crosstalk at the spatial (de)multiplexers and energy spread between discrete modal peaks are due to light propagates on both modes corresponding to distributed fiber coupling over the length of the fiber. For instance, in LP_{01} - LP_{11b} cell of the matrix, a small modal peak detected on the left is a LP_{01} impulse peak as it arrives at the same time with LP_{01} impulse in LP_{01} - LP_{01} cell. This means that when launching LP_{11b} , a small amount of LP_{01} is excited and detected by the spatial de-multiplexer receiving LP_{01} . This is a result of cross-coupling from LP_{11} to LP_{01} at the spatial multiplexer. Similarly, a small modal peak on the right in the LP_{01} - LP_{11b} cell is due to crosstalk at the spatial de-multiplexer. The energy plateau between the left and right peaks results from distributed mode coupling from the fiber between the two mode groups during the propagation. From the measured temporal-domain mode transfer matrix in Fig. 3(a), we can observe that there are relatively strong discrete cross-coupling between LP_{11} and LP_{21} mode-groups at spatial multiplexer and de-multiplexer. The maximum crosstalk occurred at spatial multiplexer and at spatial de-multiplexer were measured as -13.7 dB and -14.5 dB respectively. The magnitudes of impulses between the modal peaks resulting from distributed mode-coupling in the GI-RCF are all below -35 dB, which indicates distributed mode-coupling from the transmission GI-RCF is much weaker than the discrete modal crosstalk. In the LP_{11} - LP_{11} cells, the slope of the plateau towards to the LP_{21} modal peak is steeper than the slope of the plateau towards to the LP_{01} modal peaks, which suggests that distributed mode-coupling between LP_{01} and LP_{11} is stronger than that between LP_{11} and LP_{21} . This is because of the GI-RCF design whose Δn_{eff} between LP_{01} and LP_{11} mode-groups is smaller than that between LP_{11} and LP_{21} mode-groups and it is also reflected in the DGD measurement shown in Fig. 3(c).

3. All-optical mode-group division multiplexing over the GI-RCF

3.1 Mode channel characterization

Enabled by reconfigurable SLM based spatial (de)multiplexers, we can characterize optical mode cross-coupling property of each channel that maps one input SMF port to one output SMF port individually by measuring complex mode transfer matrix of each channel with a power meter [18]. This is necessary because different channel mappings may have different modal cross-coupling properties given that different input/output SMF ports have different offsets from the optical axis. Offsets beyond a certain limit (paraxial approximation) suffer spatial varying off-axis optical aberrations/distortions from the conventional lens. The mode transfer matrix at a wavelength describes linear behavior of an optical system mapping any input optical field with resultant output field at the other end. During the mode channel characterization, we use a filtered and polarized amplified spontaneous emission source (0.5nm at 1545.54nm) to approximate a high bandwidth channel. The fiber arrays installed at the SLM based spatial (de)multiplexers have seven SMF ports and therefore the SLM based spatial (de)multiplexers support up to seven mode/mode-group channels. We individually measured optical mode transfer matrix of each of all supported channels to study mode-coupling properties between different supported channels. We find that all the channels have nearly identical mode-coupling properties indicated by almost the same power distributions in their mode transfer matrices shown as an example in Fig. 4. This enables us to reroute or add/drop any mode or mode-groups from/to available input/output SMF ports by programming the SLMs due to the identical mode-coupling properties among different channels. In comparison with [14], optical distortions induced by large spacing (250 μ m) multiple-fiber push-on (MPO) connectors are much reduced by using SMF arrays with smaller spacing (50 μ m) at SLM based spatial (de)multiplexers. Figure 4 exhibits power distribution of measured optical mode transfer matrix of a typical channel over the 360m GI-RCF. Among all mode channels, modal crosstalk between any adjacent mode-groups is in the range of from -14.2dB but to -10.6dB and modal crosstalk between the two non-adjacent mode-groups is less than -20dB. Relatively weak coupling between mode-groups shown in the mode transfer matrix enables multiplexing and demultiplexing mode-groups all-optically without significant performance penalties.

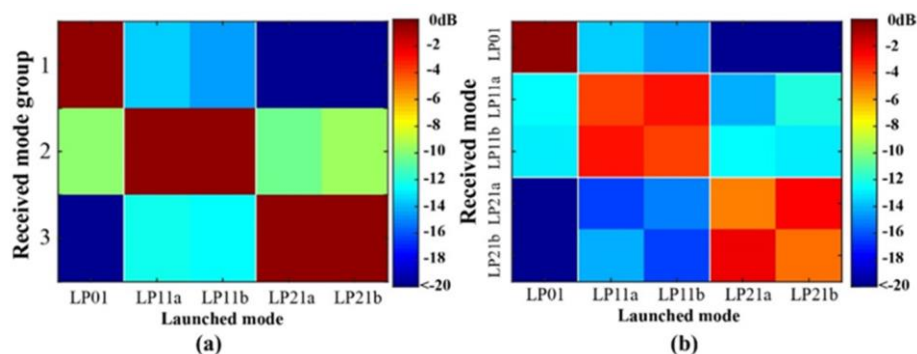


Fig. 4. Power distributions (a) aggregated and (b) non-aggregated by mode group of measured optical mode transfer matrix of a typical channel over the 360 m GI-RCF.

3.2 Reconfigurable all-optical mode-group division multiplexing

In mode-multiplexing operations, multichannel composite phase masks are constructed at the SLM based spatial (de)multiplexers to multiplex/demultiplex different distributions of modes from/to different input/output SMF ports using a basis library that consists of the phase masks for precisely launching/detecting each mode of the GI-RCF. The multichannel phase mask for

one polarization is constructed by superposing phase masks for each individual modal channel and each individual channel's phase mask is a superposition of complex distribution of all constituent modes propagating on that channel and a tilted wavefront that directs the illuminating beam in its corresponding direction with optical aberration correction represented by Zernike polynomials [19]. In this mode-group multiplexing demonstration, independent Gaussian beams with their corresponding incidence angles illuminate the composite phase mask for each polarization at the SLM multiplexer and each Gaussian beam accurately excites a mode in a different mode-group in two polarizations. At the receiving end of the fiber, relative amplitude and phase of all degenerate modes in each of used mode-groups for each polarization are measured first and this information is then used to route the modal distribution of each multiplexed mode-group to its assigned output SMF port. Although the SLM based spatial (de)multiplexers support polarization division multiplexing (PDM), this work here focus on pure mode-group division multiplexing without combining PDM and polarization diversity information is not measured in the experiments. Two polarization components of each demultiplexed modal channel are combined to the same output SMF port. The phase marks are reconfigurable and can dynamically adjust relative attenuation of each modal channel by assigning an optimized weighting factor to compensate mode dependent loss and equalize received optical power between all modal channels.

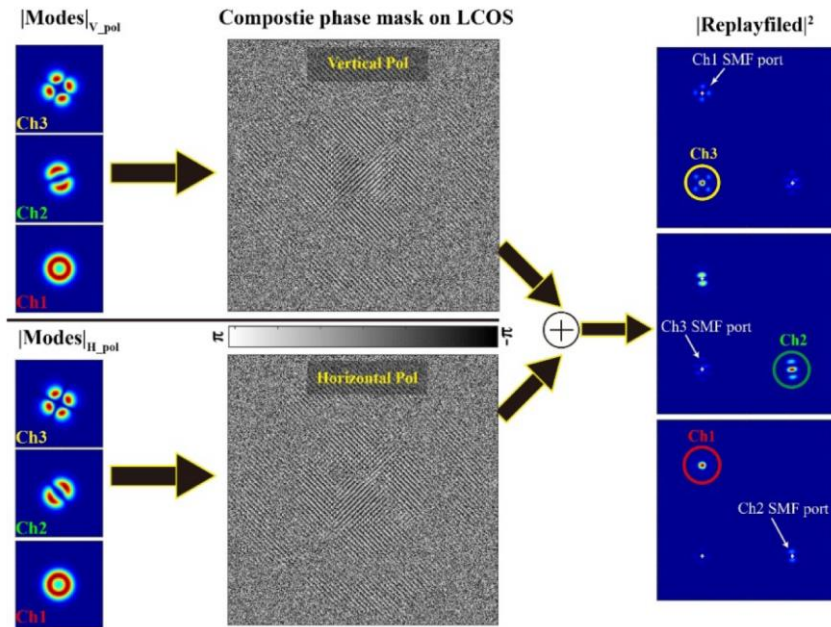


Fig. 5. Simulated visualization of all-optical demultiplexing modal distribution of each mode-group channel to its assigned output SMF port in the full (three) mode-group multiplexed transmission experiment over the GI-RCF. White crosshairs show the positions of optical axes of output SMF ports.

Figure 5 visually illustrates all-optical de-multiplexing operation performed by the SLM based spatial de-multiplexer displaying constructed composite phase masks for two polarizations in the three mode-group multiplexed transmission over the GI-RCF experiment. At the SLM de-multiplexer, launched LP_{01} mode arrives mostly intact with random polarization mixing, whereas launched LP_{11a} or LP_{21a} mode arrives as a random superposition of degenerate modes in each corresponding mode-group with random polarization mixing. The composite phase masks detect the measured modal distributions of each of the three mode-groups in two polarizations and direct them to each assigned output SMF port that corresponds to a spatial position in the replay field. We can see that in the replay field not

only do formed autocorrelation peaks (within colored circles in Fig. 5) cover on the target SMF ports but also there are formed cross-correlation distributions surrounding the other channels' output SMF ports. This results from superposing phase masks of each channel to construct the multichannel composite phase mask and there is a loss associated with the superposition. We also observe that the intensities of the formed cross-correlation distributions near the LP₀₁ (Ch1) and LP₁₁ (Ch2) output SMF ports are relatively stronger when respectively demultiplexing LP₁₁ and LP₀₁ mode-groups, which indicates relatively higher splitting loss. This is because there is a relatively big intensity overlap between LP₀₁ and LP₁₁ mode of the GI-RCF. LP₂₁ mode that propagates much closer to the outer cladding of the GI-RCF has small intensity overlaps with LP₀₁ and LP₁₁ mode that propagate near the inner cladding of the GI-RCF. Therefore, the multichannel composite phase mask performs a more efficient split between LP₂₁ and the other modes. The intensity diversity between the modes can also be observed from the structure of the composite phase mask, the inner, middle and outer region of which are respectively of the form of the LP₀₁, LP₁₁, and LP₂₁ phase masks.

3.3 Data transmission performance

The experimental system used for the data transmission test is shown in Fig. 6. It is comprised of the transmitter, SLM based spatial (de)multiplexers, the transmission GI-RCF and the receiver. An Anritsu MP1800A bit error rate tester (BERT) was used for both pulse pattern generation and error detection. A Mach-Zehnder modulator driven by the BERT modulates a 1550 nm laser to generate a 12.5Gbps non-return-to-zero (NRZ) $2^{31}-1$ pseudo random binary sequence (PRBS) data pattern. The signal is then split into three tributaries that are decorrelated with large relative delays. These three decorrelated signals are accurately launched into the LP₀₁, LP_{11a} and LP_{21a} mode of the GI-RCF. After transmission over the 360m GI-RCF, the SLM de-multiplexer measures complex coefficients of all degenerate modes in each of the three mode-groups in each polarization given the mode launch and uses this information to construct three-channel composite phase masks to demultiplex each mode-group channel to its desired output SMF port. The weighting of each channel in the composite phase mask is optimized through an iterative feedback algorithm to equalize received optical power and minimize crosstalk between channels. A photo-detector connected back to the BERT system was used to sequentially measure the BER performance of each channel as a function of the received optical power.

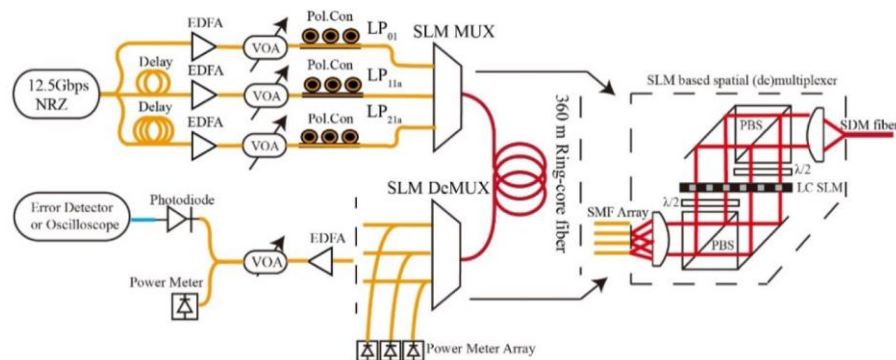


Fig. 6. Mode-group division multiplexing system that optically multiplexes three spatial mode-groups from separate input SMF ports into the GI-RCF and de-multiplexes the mode-group channels to separate output SMF ports.

We performed two sets of mode-group division multiplexing over the GI-RCF: three mode-group multiplexed transmission using all supported mode-groups and two mode-group multiplexed transmission using the two non-adjacent mode-groups. Figure 7 presents

measured BER performance as a function of the received optical power for these experiments. In the three mode-group multiplexing experiment, the measured overall optical leakage to each channel from the other two channels was -12.6dB at the start of the BER measurements. We achieve BER below the hard-decision forward error correction (FEC) threshold (3.8×10^{-3}) for the three mode-group multiplexed channels and the required power penalty at the FEC threshold were 1.8dB over single-channel operation for all three channels because of residual crosstalk between mode-group channels. In the two mode-group multiplexed transmission experiment, the optical path for LP_{11a} was disconnected from the system shown in Fig. 6 and the reconfigurable SLM based spatial (de)multiplexers are programmed with two-channel composite phase masks at both ends for multiplexing and demultiplexing the two mode-group channels. The optical isolation between the two modal channels were measured as 20dB . Error free ($\text{BER} < 10^{-12}$) data transmission was achieved in the two mode-group multiplexing experiment. The two mode-group multiplexing operation suffers 1.1dB power penalty over single channel operation at a BER of 10^{-12} .

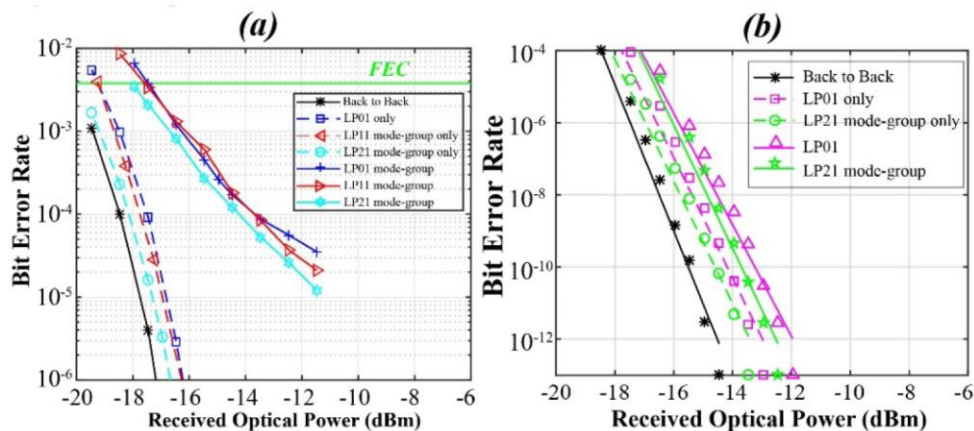


Fig. 7. Measured BER curves versus received optical power at 12.5Gbps NRZ: (a) three mode-group multiplexed transmission over the GI-RCF using all supported mode-groups, and (b) two mode-group multiplexed transmission using the two non-adjacent mode-groups.

4. Conclusion

Reconfigurable SLM based spatial (de)multiplexers are flexible and can adapt different types of SDM fibers by programming with appropriate phase masks. Using the SLM based spatial (de)multiplexers, we have successfully demonstrated all-optical mode-group multiplexed transmissions over a customized 360m graded-index ring-core fiber supporting 3 LP mode-groups without MIMO processing employing either all supported three mode-groups or the two non-adjacent mode-groups. Weak coupling between employed mode-groups enables us to achieve BER far below the FEC threshold in the three mode-group multiplexed transmission ($3 \times 12.5\text{Gbps}$ NRZ) and error free ($\text{BER} < 10^{-12}$) in the two mode-group multiplexed transmission ($2 \times 12.5\text{Gbps}$ NRZ). Resultant power penalties over single channel operations were respectively 1.8dB at the FEC threshold for the 3 mode-group multiplexing and 1.1dB at a BER of 10^{-12} for the 2 mode-group multiplexing. Detailed modal cross-coupling properties of the customized graded-index ring-core fiber are also characterized by measuring complex mode transfer matrix.

Funding

The UK Engineering and Physical Sciences Research Council (EPSRC) grant: EP/J009369/1 (COMIMO); a Cambridge University EPSRC Impact Acceleration Account (IAA) follow-on grant.